Astron. Astrophys. 361, 451–464 (2000)

ASTRONOMY AND ASTROPHYSICS

The influence of interactions and minor mergers on the structure of galactic disks⋆

II. Results and interpretations

U. Schwarzkopf[1,2,⋆⋆] **and R.-J. Dettmar**[1]

[1] Astronomisches Institut, Ruhr-Universität Bochum, Universitätsstrasse 150, 44780 Bochum, Germany
[2] Steward Observatory, University of Arizona, 933 N. Cherry Ave., Tucson, Arizona 85721, USA

Received 13 September 1999 / Accepted 15 June 2000

Abstract. We present the second part of a detailed statistical study focussed on the effects of tidal interactions and minor mergers on the radial and vertical disk structure of spiral galaxies. In the first part we reported on the sample selection, observations, and applied disk models. In this paper the results are presented, based on disk parameters derived from a sample of 110 highly-inclined/edge-on galaxies. This sample consists of two subsamples of 49 interacting/merging and 61 non-interacting galaxies. Additionally, 41 of these galaxies were observed in the NIR. We find significant changes of the disk structure in vertical direction, resulting in ≈ 1.5 times larger scale heights and thus vertical velocity dispersions. The radial disk structure, characterized by the cut-off radius and the scale length, shows no statistically significant changes. Thus, the ratio of radial to vertical scale parameters, h/z_0, is ≈ 1.7 times smaller for the sample of interacting/merging galaxies. The total lack of typical flat disk ratios $h/z_0 > 7$ in the latter sample implies that vertical disk heating is most efficient for (extremely) thin disks. Statistically nearly all galactic disks in the sample (93%) possess non-isothermal vertical luminosity profiles like the sech (60%) and exp (33%) distribution, independent of the sample and passband investigated. This indicates that, in spite of tidal perturbations and disk thickening, the initial vertical distribution of disk stars is not destroyed by interactions or minor mergers.

Key words: galaxies: evolution – galaxies: general – galaxies: interactions – galaxies: kinematics and dynamics – galaxies: photometry – infrared: galaxies

Send offprint requests to: U. Schwarzkopf (schwarz@as.arizona.edu)

⋆ Based on observations obtained at the European Southern Observatory (ESO, La Silla, Chile), Calar Alto Observatory operated by the MPIA (DSAZ, Spain), Lowell Observatory (Flagstaff/AZ, USA), and Hoher List Observatory (Germany).

⋆⋆ *Present address:* Steward Observatory, University of Arizona, 933 N. Cherry Ave., Tucson, Arizona 85721, USA

1. Introduction

Although major galaxy mergers seem to be more spectacular and have therefore received the most attention, there is evidence that tidal interactions or the accretion of small, low-mass satellites ("minor mergers") occur more frequently in the local universe (e.g. Frenk et al. 1988; Carlberg & Couchman 1989). Considering the high density of galaxies in groups and clusters and the fact that a large fraction of their members belongs to the dwarf galaxy population it is not unexpected that we know a large number of galaxies influenced by environmental effects of this order of magnitude. That includes both galaxies with clear signs of tidal interactions that happend in the recent past and those currently involved merging processes (Arp 1966; Arp & Madore 1987; Fried 1988; Zaritsky et al. 1993, 1997). A good example is our own Galaxy, that forms a future minor merger together with the Large Magellanic Cloud ($M_{\rm LMC} \approx 2 \times 10^{10}\ M_\odot$; $M_{\rm LMC}/M_{\rm MW} \approx 0.1$) and with several other satellites (e.g. Sgr dwarf elliptical) having smaller mass ratios (Irwin et al. 1985; Schommer et al. 1992; Toth & Ostriker 1992; Ibata & Lewis 1998). However, little is known about the rate of minor merging events, their influence on the structure and kinematics of galactic disks, and the efficiency of evoked perturbations.

In recent years this problem has been addressed by several numerical N-body simulations as well as analytical estimations. It was found that minor mergers and accretion events in the range $M_{\rm sat}/M_{\rm disk} \approx 0.05 \ldots 0.2$ must be a more common processes in the local universe than previously argued, representing an important mechanism for driving the evolution of galaxies. In particular, it was concluded that one of the most striking structural changes produced by a single merger is a vertical disk thickening by a factor of 2–4, dependending noticeably on the initial disk properties such as the ratio between scale length and -height h/z_0 (Ostriker 1990; Toth & Ostriker 1992; Quinn et al. 1993; Mihos et al. 1995; Walker et al. 1996). However, the self-consistent simulations recently carried out by Velazquez & White (1999) indicate that these results tend to overestimate the vertical disk heating. They find that the heating factor is closer to 1.5–2, depending mainly on the satellite orbit (i.e. prograde or

retrograde) and the mass of the bulge component. Furthermore, the obtained results might still be influenced by counteracting processes such as dissipative gas cooling, subsequent star formation, the presence of several stellar disk components, etc. On the other hand, the observed thinness of typical late-type galaxy disks without indications of tidal interaction/accretion constrains the value of vertical disk heating. It is thus unlikely that such "superthin" galaxies have absorbed more than a few percent of their mass within their lifetime (Toth & Ostriker 1992).

At present there are only a few observational studies that aim at proving the effects predicted by the simulations. Zaritsky (1995) analyzed observations of nearby spiral galaxies based on magnitude residuals from the Tully-Fisher relationship, chemical abundance gradients, and asymmetries in their stellar disks. He concluded that even relatively isolated spiral galaxies have experienced accretion of companion galaxies over the last few Gigayears. In their series of studies Reshetnikov et al. (1993) and Reshetnikov & Combes (1996, 1997) investigated the effects of tidally-triggered disk thickening between galaxies of comparable mass. They used optical photometric data of a sample of 24 interacting/merging and a control sample of 7 non-interacting disk galaxies. As a main result they find that the ratio h/z_0 of the radial exponential disk scale length h to the constant scale height z_0 is about two times smaller for interacting galaxies. However, the relatively small galaxy samples used in these studies make it difficult to derive reliable estimates on the actual size of the structural changes. This also prevents a consistent check with the results from simulations.

Therefore we started a detailed statistical study in order to investigate systematically the influence of interactions and minor mergers on the radial and vertical disk structure of spiral galaxies in both optical and near infrared (NIR) passbands. Our study is based on a sample of 110 highly-inclined/edge-on disk galaxies, consisting of two subsamples of 61 non-interacting galaxies and 49 interacting/minor merger candidates. Additionally, 41 of these galaxies were observed in the NIR.

In Paper I (Schwarzkopf & Dettmar 2000a) a detailed description of the project structure and its main questions was given. We reported on the sample selection, observations, and data reduction as well as on the disk modelling- and fitting procedure.

In Sect. 2 of this paper (Paper II) the sample and applied corrections are briefly summarized. In Sect. 3 we analyze the radial and vertical disk structure of both subsamples. The global disk parameters, their ratios, and the vertical brightness distribution are investigated. The derived colour gradients are also analyzed. We discuss the obtained results in Sect. 4 and summarize and conclude the paper in Sect. 5.

2. The data

2.1. Sample and observations

In Paper I we found that it is crucial for this study to have two subsamples of highly-inclined/edge-on galaxies ($i \geq 85°$) that were selected carefully in order to diminish overlapping effects, i.e. a contamination introduced by an uncertain allocation of galaxies to the non-interacting or interacting/merging sample. For the latter sample we therefore used a classification scheme that was introduced by Arp & Madore (1987). Additionally, for most of the minor merger candidates the mass ratio between the companion and the main body was checked. Finally, we have shown that the distribution of the morphological types between both subsamples is statistically indistinguishable over the whole range studied, i.e. between $0 \leq T \leq 9$ (Paper I). Although we cannot exclude overlapping effects completely, the remaining uncertainties in the classification of the subsamples were thus reduced to a minimum. A wrong allocation of objects would only lead to an underestimation of the actual differences between both samples.

Since a large sample of galaxies was needed for this study the observations were obtained with different telescopes and during several observing runs between February 1996 and June 1998. Details of the observations and the data reduction can also be found in Paper I.

2.2. Distances and corrections

The distances to the observed galaxies with known redshifts were calculated using a Hubble flow with a Hubble constant of $H_0 = 75\,\mathrm{km\,s^{-1}Mpc^{-1}}$, corrected for the "Virgocentric Flow" model predicted by Kraan-Korteweg (1986). The model chosen is characterized by a local infall motion of the Local Group towards the Virgo cluster with an adopted velocity of $v_{\mathrm{vc}} = 220\,\mathrm{km\,s^{-1}}$. It describes the motions of galaxies in the environment of the cluster by a non-linear flow-model. Assuming this model and the adopted Hubble constant, the distance of the Virgo cluster is $r_{\mathrm{vir}} = 15.8$ Mpc.

The heliocentric velocities v_0 needed for this model are listed in Table 5, Column (5). They were calculated from optical/HI-velocities taken from NED[1]. The heliocentric velocities v_0 were corrected for the system velocity v_{LG} of the Local Group via formula (2) in Richter et al. (1987). The velocity corrections Δv required for this model were derived from Fig. 3a in Kraan-Korteweg (1986).

The distance distribution of all sample galaxies with known redshifts ($n = 97$) is shown in Fig. 1a. The nearest galaxy is NGC 4244 at 3.8 Mpc, the most distant galaxy is ESO 379-G20 at 193 Mpc (Table 5). Fig. 1b shows the distance distributions for both subsamples of 43 interacting/merging and 54 non-interacting galaxies. According to the test of Kolmogorov & Smirnov (Darling 1957; Sachs 1992) – hereafter KS – both distributions are statistically indistinguishable: the test result of 0.09 is significantly lower than the value necessary for the 20%-limit (0.22), which is the strongest of the KS-criteria. This is – in addition to the indistinguishable distribution of morphological types (Paper I, Fig. 1) – essential in order to avoid selection biases and thus to derive reliable disk parameters.

[1] The NASA/IPAC Extragalactic Database (NED) is operated by the Jet Propulsion Laboratory, California Institute of Technology, under contract with the National Aeronautics and Space Administration.

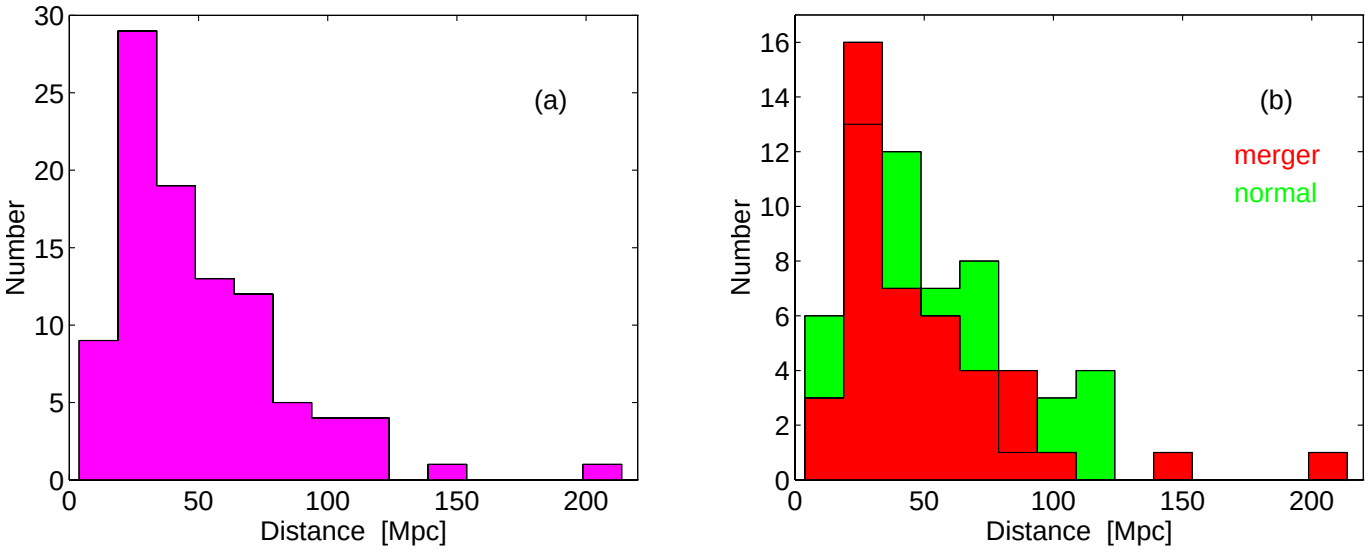

Fig. 1a and b. The distribution of distances **a** for the total galaxy sample, and **b** for both subsamples of non-interacting (normal) and interacting/merging galaxies (all distances are corrected for Virgo infall).

Since seeing effects become significant for small disk structures such as the scale height of flat disks (for seeing conditions around $2''$ and for features $\leq 4''$ the error amounts to 20%) all disk parameters listed in Table 5 were corrected in the following way: using the values of predominant seeing conditions (derived from averaged FWHM values of stars in the resulting frames, given in Paper I, Table 2) the images were de-convoluted with the Lucy-Richardson algorithm (standard MIDAS routine). In order to profit from the full vertical resolution – important to distinguish between different vertical disk models used for fitting; Paper I, Sect. 4) – no vertical binning was applied.

2.3. Disk models and fitting procedure

In order to analyze and to compare the structure of disk components of a large sample of highly-inclined/edge-on spiral galaxies we developed an improved disk modelling- and fitting procedure that is based on a 3-dimensional luminosity distribution proposed by van der Kruit & Searle (1981a, b; 1982a), hereafter KS I–III. The results presented in the next section were derived using these disk models. An detailed description of their properties and the determination of global disk parameters was given in Paper I.

3. Results

The following statistical analysis compares the radial and vertical disk parameters of both galaxy samples based on the optical (R-band) data set. The derived main disk parameters are: inclination angle i, cut-off radius $R_{\rm max}$, scale length h, scale height z_0, and best-fitting vertical model $f(z)$. They are listed in Table 5, Columns (7)-(11).

3.1. The radial and vertical disk structure

3.1.1. The cut-off radius "$R_{\rm max}$"

The distribution of disk cut-off radii derived from the values in Table 5 is shown in Fig. 2 for the samples of non-interacting and interacting/merging galaxies. Both distributions cover a wide range between 4 kpc $\leq R_{\rm max} \leq$ 45 kpc, with the same global maximum around ≈ 14 kpc. Slight differences can be detected in a region of large cut-off radii: many of the interacting/merging galaxy disks are concentrated in a strong peak between 8 kpc $\leq R_{\rm max} \leq$ 16 kpc, followed by a noticable drop-off towards larger radii. The distribution ends abruptly at $R_{\rm max} \approx 32$ kpc.

Disks of non-interacting galaxies show a more regular distribution, decreasing from the maximum at $R_{\rm max} = 14$ kpc towards larger radii. However, the median derived for both distributions is almost identical at $(R_{\rm max})_{\rm norm.} \approx 17.2$ kpc and $(R_{\rm max})_{\rm merg.} \approx 17.0$ kpc, respectively.

Since the slight differences detected between the two distributions are caused by only a few galaxies, the KS-test shows that both samples are close to unity and thus statistically indistinguishable (the result of 0.14 is clearly below the critical 20%-limit of 0.22).

3.1.2. The disk scale length "h"

In Fig. 3 the distribution of disk scale lengths is shown for the non-interacting and interacting/merging galaxy samples. As in the cut-off statistics, both distributions have approximately the same global maxima, located at $h \approx 4$ kpc. The disks of non-interacting galaxies possess scale lengths in a wide range between 1.5 kpc $\leq h \leq$ 16 kpc, with a regular decrease towards larger values. The distribution of disk scale lengths of interacting spirals shows a similar behaviour, but with a more sharply

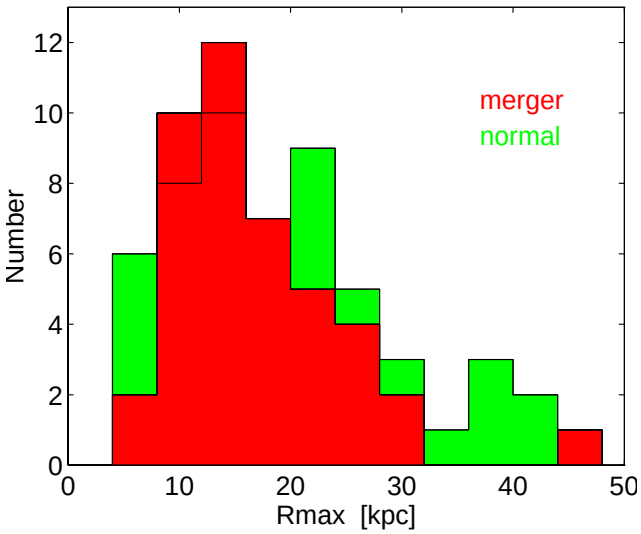

Fig. 2. The distribution of disk cut-off radii for the sample of non-interacting and interacting/merging galaxies.

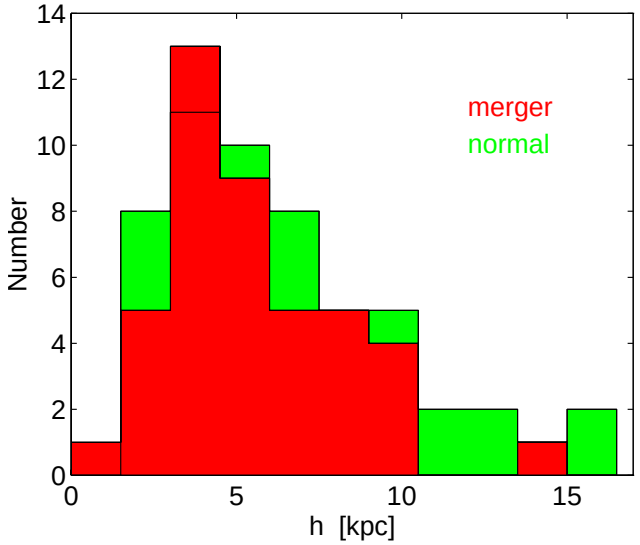

Fig. 3. The distribution of disk scale lengths for the sample of non-interacting and interacting/merging galaxies.

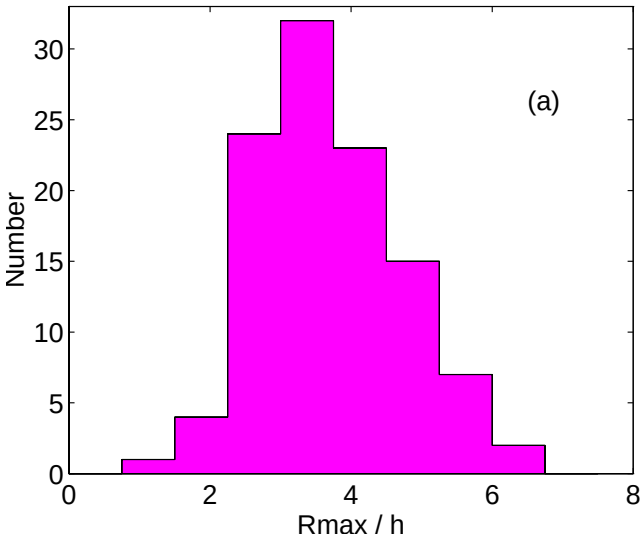

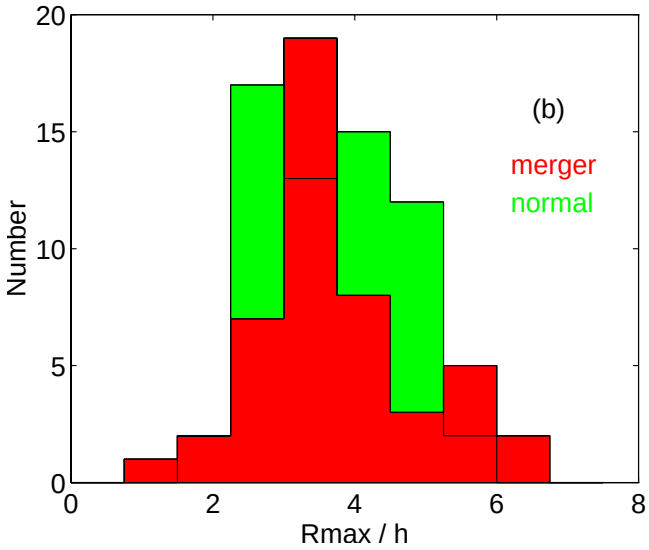

Fig. 4a and b. Ratio of radial disk parameters $R_{\max}/h$ **a** for the total galaxy sample, and **b** for normal/interacting galaxies.

truncated end at $h \approx 10.5$ kpc. This results in a slightly different median for both distributions at $h_{\rm norm.} \approx 5.6$ kpc and $h_{\rm merg.} \approx 4.9$ kpc, respectively.

In analogy to the cut-off-statistics, the differences between both h-distributions are only due to a few galaxies (most probably reflecting the slightly different number of galaxies in both samples) and thus marginal. The KS-test therefore classifies these differences as statistically insignificant with a result of 0.11, which is clearly below the mentioned 20%-limit of 0.22.

3.1.3. The ratio of radial parameters "$R_{\max}/h$"

Although several studies of edge-on spiral galaxies were focussed on an investigation of disk scale parameters of non-interacting galaxies, only a few have studied the ratio of disk cut-off radius to the scale length $R_{\max}/h$ (KS I-III; Barnaby & Thronson 1992; Barteldrees & Dettmar 1994; Schwarzkopf 1999; Schwarzkopf & Dettmar 1997). One of the reasons might be the fact that for most purposes a disk model consisting of a radial exponentially decreasing luminosity without a cut-off may be a good approximation (Shaw & Gilmore 1989; de Grijs & van der Kruit 1996; de Grijs et al. 1997; Reshetnikow & Combes 1996, 1997). However, the importance of a cut-off radius as a reasonable step towards a more realistic description of the properties of galactic disks and its necessity for a precise quantitative description of the observed radial disk profiles were impressively confirmed by the results of the former studies. The existence of a disk cut-off, although still objectionable within the framework of galaxy evolution, seems therefore now well accepted.

Table 1. Comparison of radial disk parameter ratios $R_{\max}/h$ (this study and literature data). Columns: (1) Source: KS I–III= van der Kruit & Searle (1981a, b; 1982a); K= van der Kruit (1986); H=Habing (1988); SG= Shaw & Gilmore (1989); G= Gilmore et al. (1989); BT= Barnaby & Thronson (1992); BD= Barteldrees & Dettmar (1994); SD I= Schwarzkopf & Dettmar (1997); SD II= this study; (2) Ratio $R_{\max}/h$ and error; (3) Absolute range of $R_{\max}$; (4) Mean value of Column (3); (5) Number of galaxies used; (6) Range of morph galaxy types; (7) Distance range of sample galaxies.

Source	$R_{\max}/h$	$R_{\max}$ [kpc]	$\overline{R}_{\max}$ [kpc]	Sample	Type	Dist [Mpc]
(1)	(2)	(3)	(4)	(5)	(6)	(7)
KS I–III	4.25 ± 0.6	7.8 – 24.9	17.1	8	3.0 – 6.0	5.0 – 14.0
K, H, SG, G	4.20 ± 1.0	18.0	18.0	Galaxy	4.0	–
BT	3.38	19.3	19.3	NGC 5907	6.0	11.0
BD	3.70 ± 1.0	10.5 – 38.9	20.2	27	0.0 – 7.0	26.0 – 113.0
SD I	3.61 ± 0.9	10.5 – 37.8	19.4	37	-2.0 – 6.3	25.0 – 162.9
SD II (total sample)[a)]	3.59 ± 0.6	2.9 – 45.5	17.2	108	0 – 9.0	3.8 – 193.0
SD II (non-interacting)[a)]	3.66 ± 0.7	4.2 – 40.9	17.2	61	0 – 9.0	3.8 – 114.4
SD II (interacting/merging)[a)]	3.53 ± 0.6	2.9 – 45.5	17.0	47	0 – 9.0	4.8 – 193.0

[a)] Optical (R-band) data.

This is consistent with the results of our disk modelling procedure (Paper I), showing that the shape of radial disk profiles and thus the derived value for the disk scale length is also influenced by the size of the cut-off radius. Using a disk model without a cut-off would increase the (existing) uncertainties in estimating reliable disk scale lengths.

The ratios $R_{\max}/h$ found in this study for both samples of non-interacting and interacting/merging galaxies are summarized in Table 1. They are compared with the data from literature of published samples of non-interacting galaxies. Fig. 4 shows the $R_{\max}/h$-distribution for both the total galaxy sample and the two subsamples. Due to its statistically significance (108 galaxies) the distribution of the total galaxy sample is very regular and, though the slightly steeper drop-off towards smaller values, close to a Gaussian. The median of the total sample is at $(R_{\max}/h)_{\rm tot} = 3.59$, that of the non-interacting and interacting/merging galaxy sample at $(R_{\max}/h)_{\rm norm.} = 3.66$ and $(R_{\max}/h)_{\rm merg.} = 3.53$, respectively (typical errors are given in Table 1). According to the KS-test both distributions are statistically indistinguishable with a result of 0.12 (critical 20%-limit is at 0.21).

The relatively high scatter of the merger-sample, which becomes apparent in a wider basis of the distribution (Fig. 4b), is mainly due to a radially perturbed disk structure of these galaxies. These perturbations may cause asymmetries in the radial disk profiles and thus substantially errors in the scale length and/or the cut-off radius. Unlike this result it is a remarkable fact that the $R_{\max}/h$-distribution of interacting/merging galaxies shows a very sharp peak at $R_{\max}/h \approx 3.4$, while non-interacting galaxies are spread in a much wider plateau.

Within the estimated errors the obtained $R_{\max}/h$-ratios of all (sub-)samples are consistent with other studies (Table 1). However, this study – dealing with the by far largest galaxy sample for a cut-off statistics and hence with smaller errors – indicates that the $R_{\max}/h$-ratios are lower than previously argued. The mean ratio now seems to be closer to $(R_{\max}/h)_{\rm tot} = 3.6$ than to the value 4.2 often used in the literature. This fact may be explained by selection effects of studies dealing with statistically very small samples of relatively nearby ($D \leq 20$ Mpc) and medium-sized ($R_{\max} \leq 25$ kpc) galaxies, which is the case for some of these data. Therefore, some additional information on these studies are included in Table 1. A possible correlation between disk parameters and distance will be studied in Sect. 3.2.

3.1.4. The disk scale height "z_0"

The distribution of exponential disk scale heights z_0 – calculated by using the absolute z_0-values in Table 5, Column (10), and the corresponding transformations in (5) of Paper I – is shown in Fig. 5a for the non-interacting galaxy sample, and in Fig. 5b for the interacting/merging galaxies. By comparing these diagrams clear differences concerning both the trend and the median of the distributions can be detected:

The majority ($\approx 60\%$) of normal galaxies is concentrated in a region $z_0 \leq 1.1$ kpc, with a clear maximum between 400 pc $\leq z_0 \leq$ 800 pc. The distribution shows a sharp truncation towards extremely thin disks at $z_0 = 300$ pc, followed by a very regularly decreasing part towards thicker disks up to $z_0 \approx 3$ kpc.

Unlike this, the distribution of interacting/merging galaxies shows a trend that is completely contrary to that found for normal galaxies: the scale height increases rapidly towards thicker disks, having a maximum between 1.2 kpc $\leq z_0 \leq$ 1.6 kpc, and a higher frequency of disks thicker than 2 kpc. The median for both distributions is $(z_0)_{\rm norm.} \approx 1.0$ kpc and $(z_0)_{\rm merg.} \approx 1.5$ kpc. It is also remarkable that very thin disks in the range 250 pc $\leq z_0 \leq$ 450 pc, as they are frequently observed in the sample of non-interacting galaxies (e.g. UGC 231, UGC 4278, UGC 4943, see Table 5), are completely missing in the interacting sample. Since this is not due to the sample selection criteria (Paper I) it is most likely a result of the various collective instabilities of such thin disks, in particular against external perturbations as

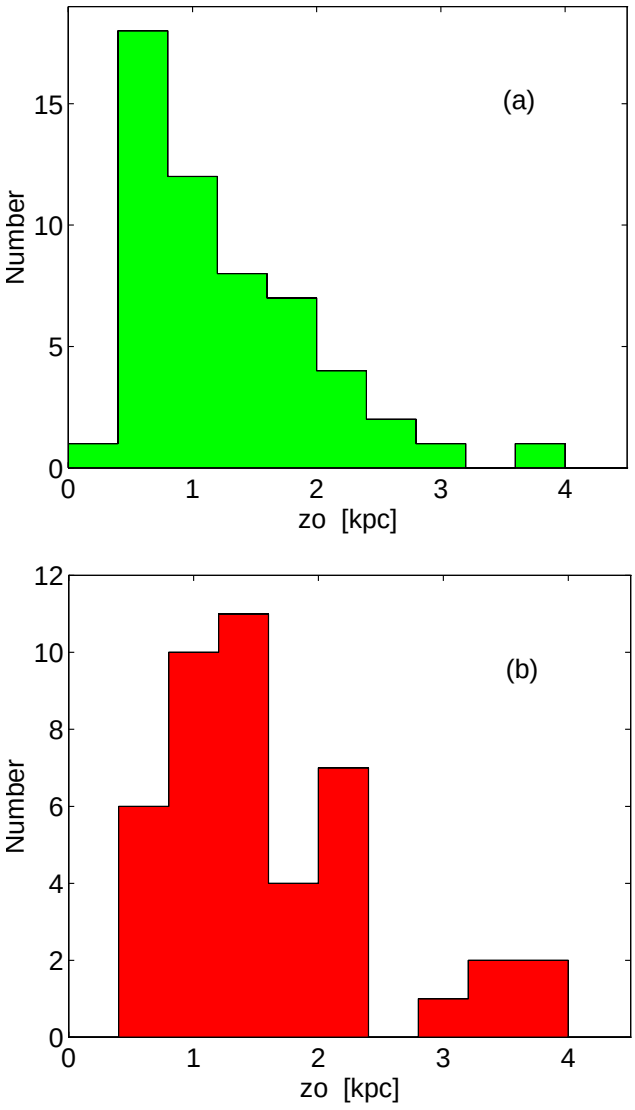

Fig. 5a and b. The distribution of disk scale heights **a** for the sample of non-interacting and **b** for interacting/merging galaxies.

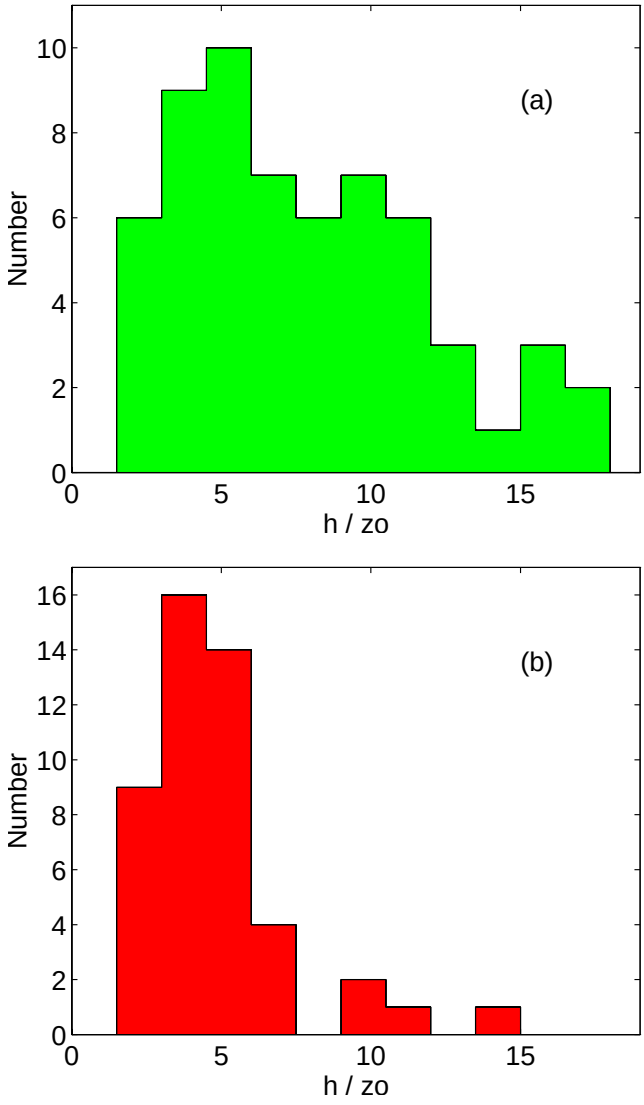

Fig. 6a and b. The ratio of radial to vertical disk parameters h/z_0 **a** for the sample of non-interacting and **b** for interacting/merging galaxies.

they are commonly evoked by tidal interactions or even minor mergers (Gerin et al. 1990; Toth & Ostriker 1992).

The KS-test confirms that the differences between both distributions are statistically significant: the result of 0.24 is above both the 20% (0.22) and the 15% (0.23) limit of the test. Since it was shown (Fig. 1 of Paper I and Sect. 2 of this paper, resp.) that the absolute disk parameters of both galaxy samples are not affected by selection biases – the distance- and type distribution were found almost indistinguishable – it can be concluded that galactic disks affected by interactions/minor mergers are ≈ 1.5 times thicker on average. We therefore infer that the disk thickening is in fact caused by the interaction or the merging process.

However, it is not yet clear whether this thickening effect was evoked only by a locally increased scale height due to a vertically perturbed disk structure or by global disk thickening. This can be clarified only after a detailed analysis of the vertical disk structure. Therefore, the behaviour of the disk scale height with radial distance, i.e. $z_0(R)$, and the effects of vertical disk perturbations will be investigated in detail in a forthcoming paper (Paper III, Schwarzkopf & Dettmar 2000c).

3.1.5. The ratio of radial to vertical parameters "h/z_0"

The ratio of radial to vertical disk scale parameters h/z_0 – hence a normalized thickness – is very suitable for characterizing and comparing the disk structure of edge-on galaxies independently of their distance. It is thus – unlike the absolute values of scale heights – more reliably for a detection of small changes in the vertical disk structure.

Fig. 6 shows the h/z_0-distribution for both samples of non-interacting and interacting/merging galaxies. As it can be seen clearly, the ratio h/z_0 for normal galaxies covers a wide range $2 \leq h/z_0 \leq 18$ between extreme thick and thin disks. Most of these galaxies are concentrated between $2 \leq h/z_0 \leq 12$, with

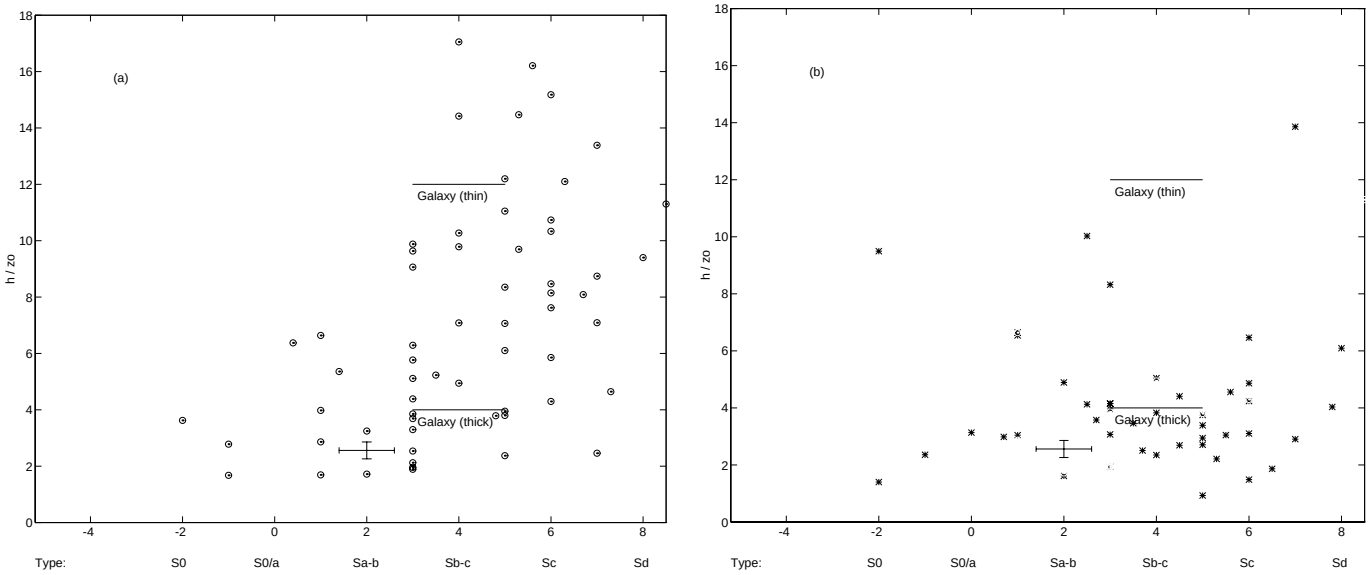

Fig. 7a and b. The dependence of ratio h/z_0 on galaxy type **a** for the sample of non-interacting galaxies. The position of the thin/thick disk component of our Galaxy as well as typical errors are indicated. Disks of interacting/merging galaxies **b** show a significant lower ratio and do not follow the h/z_0-trend of non-interacting galaxies.

a maximum at $h/z_0 \approx 5.3$. There is only a slight decrease in the number of flat disks from the maximum of the distribution towards extreme flat disk ratios, i.e. between $6 \leq h/z_0 \leq 12$.

Unlike this, the most striking feature in the h/z_0-distribution for interacting/merging galaxies is a very sharp concentration between $2 \leq h/z_0 \leq 6$, while the flat disks with ratios typically $h/z_0 > 7$ are completely missing. The distribution peaks at $h/z_0 \approx 3.7$, and there is no smooth transition towards thicker or thinner disks on both sides of this sharply truncated distribution.

The ratio of the median values for both distributions and hence a lower limit for vertical disk thickening is $(h/z_0)_{\rm norm:merg} = 7.1 : 4.3 \approx 1.7$. This factor, however, considerably underestimates the differences between both distributions due to the above mentioned lack of (extremely) thin disks ratios. The differences between both distributions are, according to the KS-test, statistically significant with a result of 0.41 even if the strongest test criterium, the 0.1%-level (limit 0.38), is used.

Together with the nearly unchanged scale lengths (Fig. 3) and the differences found between the absolute values of disk scale heights (Fig. 5) it can be concluded that vertical thickening of galactic disks affected by interactions/minor mergers amounts to $\approx 70\%$. The changes of the disk structure result mainly from an increase in scale height.

Finally, Fig. 7a shows that the ratio h/z_0 of non-interacting galaxies correlates with the morphological type of galaxies, in the sense that the disks become systematically thinner from early types (S0, $h/z_0 \approx 2 \pm 2$) to late types (Sc/Sd, $h/z_0 \approx 8 \pm 2$). Despite the relatively high intrinsic scatter, there is a smooth transition between these two extremes. It should be stressed that – due to the corrections necessary in order to compare disk scale heights derived from different vertical luminosity distributions (exp, sech, and $\rm sech^2$) – the ratio h/z_0 can be higher than 10 for some of the disks. This value represents the maximum theoretical value allowed for stable disks, derived from the so-called "maximum disk" fits (Bottema 1993). The results obtained are therefore not unexpected, and comparable ratios were also found in earlier studies (de Grijs 1997; de Grijs & van der Kruit 1996; Schwarzkopf & Dettmar 1997; Shaw & Gilmore 1989).

In contrast to this there is no such correlation between galaxy type and ratio h/z_0 for the sample of interacting/merging galaxies (Fig. 7b). The latter typically possess thickened and disturbed disks, and are therefore concentrated in the lower right part of the panel.

For comparison, the position of our Galaxy disk is also indicated in Fig. 7. The disk of the Milky Way consists presumably of both a thin and a thick component with $h/z_0 \approx 12$ and $h/z_0 \approx 4$, respectively (according to Gilmore & Reid 1983).

3.2. The dependence of disk parameters on distance

As briefly mentioned in Sect. 3.1.3 (Table 1), the samples of some previous studies seem to be biased towards nearby objects. In order to check whether the distance as a free parameter has any obvious effect on the derived disk parameters of this study, we analyzed 3 sub-samples (no differences were made between interacting and non-interacting galaxies) defined by various distance ranges (Table 2).

To ensure statistically large enough subsamples the total sample (97 galaxies) was split into three subsamples containing about 32 galaxies each. According to the non-uniform distribution of distances (Fig. 1) this leads to different distance intervals. Afterwards, the median for all disk parameters in each distance-subsample was estimated. For a better comparison, these values are also given in per cent of the median of the total sample.

Table 2. The dependence of measured disk parameters on distance and morphological galaxy type. Columns: (1) Disk parameter used for the statistics (given as median of the distance-subsample and in per cent of the median of the total sample (last column)); (2) Distance range (in Mpc), number of objects (n) within this range, and corresponding morph. galaxy type T (given as median for each subsample and the total sample, resp.).

Disk parameter[a)] (1)		Dist [Mpc] (2) 0 – 22 ($n = 32$)		22 – 45.5 ($n = 32$)		45.5 – 193 ($n = 33$)		3.8 – 193 (total sample)
		$T = 4.8 \pm 0.9$		$T = 5.1 \pm 0.9$		$T = 3.4 \pm 0.9$		$T = 3.9 \pm 0.7$
$R_{\max}$	[kpc]	11.00	(64%)	14.90	(87%)	23.50	(137%)	17.20 ± 2.6
h	[kpc]	3.58	(67%)	4.94	(93%)	7.75	(145%)	5.33 ± 0.8
z_0	[kpc]	0.98	(80%)	1.10	(89%)	1.87	(152%)	1.23 ± 0.2
$R_{\max}/h$		3.50	(97%)	3.79	(106%)	3.43	(96%)	3.59 ± 0.4
h/z_0		5.00	(93%)	5.25	(97%)	5.67	(105%)	5.40 ± 0.9

[a)] Optical (R-band) data.

Additionally, the averaged morphological galaxy type is listed for each subsample.

As can be seen in Table 2, there is a clear trend for all absolute disk parameters ($R_{\max}, h, z_0$) in the sense that their median values are increasing with distance. This behaviour reflects, however, undoubtly a selection effect and is therefore not unusual for all those studies that are using similar selection criteria: due to the limited spatially resolution of the images the selection of suitable, remote galaxies is biased towards large and bright objects, disfavouring the relative number of physically small galaxies. This is confirmed by the strikingly simultaneous trend for all absolute disk parameters listed, which goes, on average, from 70% and 90% to 145% of the median of the total sample (Table 2, values in parenthesis). In spite of this trend the distance-independent ratios $R_{\max}/h$ and h/z_0 both stay nearly constant over the whole range.

Hence, within the given errors there is no correlation between disk parameters of different distance intervals and corresponding galaxy type. Since the distance distribution of interacting and non-interacting galaxies is statistically indistinguishable (Fig. 1b), the observed selection effect applies to both samples and does therefore not influence the comparison of disk parameters derived in this study.

3.3. The vertical surface brightness distribution

The disk models applied in this study use a set of 3 different functions $f(z)$ in order to describe the luminosity distribution $L(z)$ vertically to the disk plane: $f(z) \propto$ exp, sech, and sech^2. These functions were proposed in some fundamental papers by van der Kruit & Searle (KS I-III), Wainscoat et al. (1989, 1990), and Burkert & Yoshii (1996). A detailed description of their properties as well as a comparison between different distributions were given in Sect. 4 of Paper I.

The quantitative results and experiences made in this study after fitting the disk profiles of about 150 highly-inclined/edge-on galaxies in optical and in near infrared (NIR) passbands can be summarized as follows (the complete statistics is listed in Table 3):

- A combination of 3 different luminosity distributions $f(z)$ allows a very flexible description of vertical disk profiles of all galaxies observed.
- The fit quality achieved is better than $\pm 0.^{\mathrm{m}}2$ for nearly all of the non-interacting galaxies investigated both in the optical and in NIR, even at small z.
- The fit quality of galaxy disks affected by interaction/minor merger is, in principle, comparable to that found for non-interacting galaxies. However, some galaxies in the first sample possess vertical profiles with larger deviations from an ideal disk.
- These deviations are mainly due to tidal perturbations on short scales and/or a warped disk. Such features seem to be characteristic for disks in an intermediate stage of interactions/minor mergers. A detailed study of the vertical disk structure will be given in Paper III.
- The statistics for the best-fitting vertical luminosity distribution $f(z)$ – applied to both optical and NIR disk profiles – is as follows (optical: NIR, Table 3, Columns 2–4):
  (56: 66)% $\propto$ sech; (36: 27)% $\propto$ exp; (7: 7)% $\propto \mathrm{sech}^2$.
- Thus, the vertical luminosity profiles of nearly all ($\approx 93\%$) of the galaxies are non-isothermal. In fact the profiles are more sharply peaked and preferentially somewhat closer to a sech- than to an exp-distribution.
- Statistically, the fraction of galaxies with a certain vertical luminosity profile (exp, sech, sech^2) is independent of the passband investigated (differences $< 10\%$).
- In the optical there is no fundamental difference between vertical disk profiles of non-interacting and interacting/merging galaxies.
- Accordingly, almost the same percentage of (non-interacting: interacting) galaxies shows identical vertical distributions in the optical (Table 3):
  (56: 57)% $\propto$ sech; (36: 37)% $\propto$ exp; (8: 6)% $\propto \mathrm{sech}^2$.

Table 3. Vertical surface brightness distribution of galactic disks. Columns: (1) Sample used for the statistics: total= all galaxies; non-int.= non-interacting; int./merg.= interacting/merging galaxies; (2) – (4) Number and percentage of disks with vertical luminosity distribution $\propto$ exp,- sech,- and sech^2; (5) Number of galaxies in the (sub-) sample.

Sample	Vertical Luminosity Distribution...						Number
	$\propto$ exp		$\propto$ sech		$\propto \mathrm{sech}^2$		of
	[n]	[%]	[n]	[%]	[n]	[%]	Galaxies
(1)	(2)		(3)		(4)		(5)
Optical Data							
total	40	36	62	56	8	7	110
non-int.	22	36	34	56	5	8	61
int./merg.	18	37	28	57	3	6	49
Near Infrared Data							
total	11	27	27	66	3	7	41
non-int.	7	35	11	55	2	10	20
int./merg.	4	19	16	76	1	5	21

Table 4. Optical/near infrared disk parameter ratios. Columns: (1) Sample used for the statistics; (2) – (4) Ratio (R/K) of disk cut-off radii $R_{\max}$, scale lengths h, and scale heights z_0, respectively; (5) Number of galaxies in the (sub-) sample.

Sample	Mean Ratio			Number of
	$(R_{\max})_{R/K}$	$h_{R/K}$	$(z_0)_{R/K}$	Galaxies
(1)	(2)	(3)	(4)	(5)
total	1.32 ± 0.4	1.26 ± 0.5	1.33 ± 0.4	41
non-int.	1.18 ± 0.5	1.25 ± 0.6	1.25 ± 0.5	20
int./merg.	1.47 ± 0.3	1.26 ± 0.8	1.40 ± 0.3	21

– In the NIR, interacting galaxies display preferentially sech-profiles ($76\% \propto$ sech; $19\% \propto$ exp), while in the optical this distribution is shifted towards the exp-profile ($57\% \propto$ sech; $37\% \propto$ exp).
– The results obtained are independent of the morphological type of galaxies.

3.4. Disk colour gradients

In order to analyze colour gradients derived from measurements of radial and vertical disk parameters in optical and in near infrared passbands (R/K), the mean ratios of disk cut-off radius $R_{\max}$, scale length h, and scale height z_0 – obtained for both subsamples – are listed in Table 4.

The radial and vertical disk parameters found for K and R passbands in the *total* galaxy sample indicate that the R-band values are systematically larger, i.e. of the order of $(R/K) = 1.30 \pm 0.4$. In spite of the large intrinsic scatter, comparison with literature data shows that the values (and also the errors) obtained here are consistent with gradients derived by Giovanardi & Hunt (1988) and de Grijs (1997). They found $(F/K) = 1.20 \pm 0.42$ for the F- and K passbands, and $(B/K) = 1.56 \pm 0.45$; $(I/K) = 1.19 \pm 0.17$ for the B,-I- and K passbands, respectively.

While systematically higher optical values have been found for each of the subsamples of interacting/merging $(R/K) = 1.23 \pm 0.5$ and non-interacting galaxies $(R/K) = 1.38 \pm 0.5$, the gradients of the latter sample are, however, systematically higher (Table 4).

Although the results obtained for the two subsamples are difficult to interpret, the systematic differences found for all colour gradients as well as the good agreement with other studies indicate that these gradients are not due to the large intrinsic errors. It should, however, be stressed that the low S/N ratio in the outskirts of disks of a number of faint galaxies obtained in the near infrared largely prevents a precise determination of the cut-off radius $R_{\max}$. Longer intergration times than the typical 30–40 min (on source) would be therefore necessary in order to derive more reliable values.

4. Discussion

Considering the small mass ratio between merging satellites and disks investigated here – $M_{\mathrm{sat}}/M_{\mathrm{disk}} \approx 0.1$ – the factor found for vertical disk thickening (≈ 1.6 on average) and thus the efficiency of vertical heating is substantial. This value is, however, significantly lower than the factor of 2–4 obtained in previous studies (Reshetnikov & Combes 1996, 1997; Toth & Ostriker 1992). The differences can be explained by the different mass ratio between strongly interacting systems (galaxies of comparable mass) investigated by Reshetnikov & Combes, their simplyfied disk model (isothermal) applied to all disks and the neglect of precise disk inclination. In contrast to the set of fully self-consistent N-body simulations made recently by Velazquez & White (1999) the analysis of Toth & Ostriker (1992) ignores the coherent response of the disk and its interaction with the halo. Additionally, their assumption that the orbital energy of the satellite is deposited locally in the disk is clearly unrealistic.

In fact, the increase of disk scale height by a factor of ≈ 1.6 found in this study corresponds quite well with the value of 1.5–2 obtained by Velazquez & White (1999). However, as already mentioned by Velazquez & White (1999) and in the introduction of this study, vertical disk thickening due to a minor merger crucially depends on many other factors such as the mass and density profile of the sinking satellite, its orbit (prograde or retrograde), the content of gas deposited in the disk, and – presumably most important – on the morphological type of the galaxy. That, in turn, implies that tidally-triggered disk thickening strongly depends on the B/D ratio and hence on the initial disk thickness of the galaxy, which is characterized by the ratio h/z_0. This is confirmed by the h/z_0-statistics obtained in this study (Fig. 6), showing a total lack of thin interacting/merging galaxies with $h/z_0 > 7$. This result has some direct, important consequences on the evolution of disk galaxies on cosmological timescales (Toomre 1977; Weil et al. 1998) and

would also constrain the different scenarious discussed for disk heating (Jenkins & Binney 1990, 1991; Sanchez-Salcedo 1999; Valluri 1993). Therefore a more detailed study of the parameter space using our supplementary N-body simulations, combined with the obtained results, will be given in a forthcoming paper. The mentioned good quantitative agreement between simulation and observation, however, indicates that – in spite of the rather simple approach and the number of open questions on the details of minor merger processes – the changes of the vertical disk structure must be of this order (Kleinschmidt et al. 1999; Schwarzkopf 1999; Schwarzkopf & Dettmar 1998, 1999), i.e. somewhat lower than previously argued.

Furthermore, it is still an open question whether the radial disk structure of galaxies suffering interactions/minor mergers within the mass range studied here changes significantly. The differences between both the disk cut-off and scale length statistics obtained (10% and 20% on average, resp.) are just on the level of statistical significance and do therefore not allow for an interpretation. On the other side, there is observational evidence that radial disk shrinking is a typical aftermath of tidal interactions between galaxies with comparable masses (Reshetnikov & Combes 1996, 1997). If so, this should also apply to smaller interactions and, in particular, to minor mergers (Schwarzkopf 1999). For further clarity on this point it is therefore necessary to analyze the radial behaviour of such galactic disks in greater detail and on the basis of an expanded galaxy sample, preferably supported by N-body simulations.

The fact that nearly all galactic disks investigated (93%) possess vertical luminosity profiles which are more sharply peaked than an isothermal distribution reinforces the results of previous observational studies (e.g. de Grijs et al. 1997; Schwarzkopf & Dettmar 1997) that have ruled out the validity of the sech^2-distribution as an adequate quantitative description for most galactic disks, especially close to their plane. This fact, together with the result that almost the same percentage of interacting and non-interacting galaxies shows an identical vertical disk structure (with differences smaller than 2%, see Table 3), indicates that regional damaging effects, asymmetries or perturbations evoked by tidal interactions are non-persistent phenomena with lifetimes significantly shorter than disk thickening. Furthermore, it implies that interactions/minor mergers within the investigated mass range are not capable to destroy the initial vertical disk structure.

5. Summary and conclusions

In this work a detailed statistical study is presented in order to investigate the effects of minor mergers and tidal interactions in the range $M_{\mathrm{sat}}/M_{\mathrm{disk}} \approx 0.1$ on the radial and vertical structure of galactic disks. The fundamental disk parameters of 110 highly-inclined/edge-on disk galaxies are determined in optical and in near infrared passbands. This sample consists of two subsamples of 61 non-interacting and 49 strongly interacting/merging galaxies. Additionally, 41 of these galaxies were observed in the near infrared. The main conclusions can be summarized as follows:

1. The structural changes of galactic disks affected by interaction/low-mass satellite infall are most noticeable in the direction perpendicular to the disk plane.
2. While the majority of non-interacting galaxies possess a typical exponential disk scale height of $z_0 \approx 700$ pc, disks of minor mergers were found to be systematically thicker with $z_0 \approx 1.3$ kpc.
3. On average, galactic disks affected by interactions or minor mergers have $\approx$ 1.5 times larger scale heights and thus vertical velocity dispersions than unperturbed disks.
4. The ratio of radial to vertical scale parameters, i.e. the normalized disk thickness h/z_0, is $\approx$ 1.7 times smaller for the interacting/merging sample.
5. Ratios $h/z_0 > 7$, as they are typically for flat galaxies, are completely missing in the interacting/merging sample. This implies that vertical disk heating is most efficient for such (extremely) thin disks.
6. The radial disk structure of interacting/merging galaxies, characterized by the cut-off radius R_{max} and scale length h, shows no statistically significant changes.
7. The vertical luminosity profiles of all galactic disks investigated show the following distribution (independent of the sample and passband):
   60% $\propto$ sech; 33% $\propto$ exp; 7% $\propto \mathrm{sech}^2$.
8. Thus, the majority (93%) of galactic disks possess non-isothermal vertical luminosity profiles and is somewhat closer to a sech- than to an exp distribution.
9. There are no fundamental differences between the vertical luminosity distribution of non-interacting and interacting/merging galaxies. Hence, the intrinsic distribution of disk stars keeps largely retained during and after interactions/minor mergers.

Acknowledgements. We thank the referee of this series of papers, Dr. H. Wozniak, for his useful comments and suggestions. This work was supported by *Deutsche Forschungsgemeinschaft*, DFG, under grant no. GRK118/2. This research has made use of the NASA/IPAC Extragalactic Database (NED).

References

Arp H.C., 1966, Atlas of Peculiar Galaxies. California Institute of Technology, Pasadena
Arp H.C., Madore B.F., 1987, A Catalogue of Southern Peculiar Galaxies and Associations. Vol. I&II, Cambridge University Press
Barnaby D., Thronson Jr. Harley A., 1992, AJ 103, 41
Barteldrees A., Dettmar R.-J., 1994, A&AS 103, 475
Bottema R., 1993, A&A 275, 16
Burkert A., Yoshii Y., 1996, MNRAS 282, 1349
Carlberg R.G., Couchman H.M.P., 1989, ApJ 340, 47
Darling D.A., 1957, Ann. Math. Statist. 28, 823
Frenk C.S., White S.D.M., Davis M., 1988, ApJ 327, 507
Fried J.W., 1988, A&A 189, 42
Gerin M., Combes F., Athanassoula E., 1990, A&A 230, 37
Gilmore G., Reid N., 1983, MNRAS 202, 1025
Gilmore G., King I., Kruit P.C. van der, 1989, In: The Milky Way as a Galaxy. Geneva Observatory, Sauverny-Versoix, Switzerland
Giovanardy C., Hunt L.K., 1988, AJ 95, 408

Grijs R. de, 1997, Ph.D. Thesis, University of Groningen
Grijs R. de, Kruit P.C. van der, 1996, A&AS 117, 19
Grijs R. de, Pelletier R.F., Kruit P.C. van der, 1997, A&A 327, 986
Habing H., 1988, A&A 200, 40
Ibata R.A., Lewis G.F, 1998, ApJ 500, 575
Irwin M.J., Kunkel W.E., Demers S., 1985, Nat 318, 160
Jenkins A., Binney J., 1990, MNRAS 245, 305
Jenkins A., Binney J., 1991, In: Combes F., Casoli F. (eds.) Dynamics of Galaxies and Their Molecular Cloud Distributions. Proceedings of the 146th IAU Symposium, Paris, France, Kluwer Publ., Dordrecht, p. 400
Kleinschmidt L., Theis C., Schwarzkopf U., 1999, In: Astronomische Gesellschaft Abstract Series No. 15, p. 36
Kraan-Korteweg R.C., 1986, A&AS 66, 255
Kruit P.C. van der, 1986, A&A 157, 230
Kruit P.C. van der, Searle L., 1981a, A&A 95, 105
Kruit P.C. van der, Searle L., 1981b, A&A 95, 116
Kruit P.C. van der, Searle L., 1982a, A&A 110, 61
Mihos J.C., Walker I.R., Hernquist L., 1995, ApJ 447, L87
Ostriker J.P., 1990, In: Evolution of the Universe of Galaxies. ASP Conf. Ser. Vol. 10, ASP Publ., San Francisco, p. 23
Quinn P.J., Hernquist L., Fullagar D.P., 1993, ApJ 403, 74
Reshetnikov V.P., Combes F., 1996, A&AS 116, 417
Reshetnikov V.P., Combes F., 1997, A&A 324, 80
Reshetnikov V.P., Hagen-Thorn V.A., Yakovleva V.A., 1993, A&A 278, 351
Richter O.-G., Tammann G.A., Huchtmeier W.K., 1987, A&A 171, 33
Sachs L., 1992, Angewandte Statistik. Springer-Verlag Berlin Heidelberg
Sanchez-Salcedo F.J., 1999, MNRAS 303, 755
Schommer R.A., Olszewski E.W., Suntzeff N.B., Harris H.C., 1992, AJ 103, 447
Schwarzkopf U., 1999, Ph.D. Thesis, Ruhr-University Bochum
Schwarzkopf U., Dettmar R.-J., 1997, In: Astronomische Gesellschaft Abstract Series No. 13, 238
Schwarzkopf U., Dettmar R.-J., 1998, In: Braun J.M., Richtler T. (eds.) The Magellanic Clouds and Other Dwarf Galaxies. Shaker Publ., Aachen, p. 297
Schwarzkopf U., Dettmar R.-J., 1999, Ap&SS 265, 479
Schwarzkopf U., Dettmar R.-J., 2000a, A&AS 144, 85 (Paper I)
Schwarzkopf U., Dettmar R.-J., 2000c, A&A, subm. (Paper III)
Shaw M.A., Gilmore G., 1989, MNRAS 237, 903
Toomre A., 1977, In: Tinsley B., Larson R. (eds.) The evolution of galaxies and stellar populations. Yale University Press, New Haven, p. 401
Toth G., Ostriker J.P., 1992, ApJ 389, 5
Valluri M., 1993, ApJ 408, 57
Velazquez H., White S.D.M., 1999, MNRAS 304, 254
Wainscoat R.J., Freeman K.C., Hyland A.R., 1989, ApJ 337, 163
Wainscoat R.J., Hyland A.R., Freeman K.C., 1990, ApJ 348, 85
Walker I.R., Mihos C., Hernquist L., 1996, ApJ 460, 121
Weil M.L., Eke V.R., Efstathiou G., 1998, MNRAS 300, 773
Zaritsky D., 1995, ApJ 448, L17
Zaritsky D., Smith R., Frenk C., White S.D.M., 1993, ApJ 405, 464
Zaritsky D., Kennicutt R.C., Huchra J.P., 1994, ApJ 420, 87
Zaritsky D., Smith R., Frenk C., White S.D.M., 1997, ApJ 478, 39

Table 5. Global parameters and disk properties of the optical/near infrared galaxy samples. Columns: (1) Serial number; (2) Galaxy name; (3) Passband; (4) Revised Hubble type, based on NASA/IPAC Extragalactic Database (NED); (5) Heliocentric velocity (if available), based on NED; (6) Galaxy distances, corrected for Virgocentric Flow (Sect. 2.2), using $H_0 = 75\,\mathrm{km\,s^{-1}Mpc^{-1}}$; (7) Disk inclination; (8) Cut-off radius; (9) – (10) Radial and vertical disk parameters, in case of two-components fits both parameters are given; (11) Best-fitting vertical disk model: $1 = \exp, 2 = \mathrm{sech}, 3 = \mathrm{sech}^2$.

No.	Galaxy	Band	Type	v_0	Dist	i	$R_{\max}$		h		z_0		$f(z)$
				[km s^{-1}]	[Mpc]	[°]	[″]	[kpc]	[″]	[kpc]	[″]	[kpc]	
(1)	(2)	(3)	(4)	(5)	(6)	(7)	(8)		(9)		(10)		(11)
Interacting / Merging													
1	NGC 7	R	4.5	1497	19.8	90.0	70.9	6.81	28.8	2.76	9.2	0.88	2
2	UGC 260	R	6.0	2272	31.8	88.5	69.3	10.68	20.6	3.18	6.0	0.93	2
3	NGC 128	R	-2.0	4241	59.7	90.0	85.5	24.75	17.1	4.95	12.1	3.49	1
		K	-2.0	4241	59.7	90.0	56.3	16.30	16.0	4.63	7.4	2.15	2
4	AM 0107-375	R	3.5	—	—	90.0	24.3	—	6.9	—	2.7	—	2
5	ESO 296-G17	R	3.0	5992	83.3	89.5	53.6	21.63	18.8	7.61	6.4	2.58	2
6	ESO 354-G05	R	4.0	—	—	90.0	30.7	—	7.9	—	2.8	—	2
7	ESO 245-G10	R	3.0	5713	79.6	89.0	46.1	17.80	22.3	8.61	7.9	3.06	2
8	ESO 417-G08	R	0.7	4893	67.5	89.5	64.5	21.10	16.9	5.52	7.9	2.60	2
9	ESO 199-G12	R	8.0	6993	96.5	90.0	40.7	19.03	15.9	7.44	3.6	1.71	2
10	ESO 357-G16	R	3.0	1382	18.2	90.0	54.5	4.81	16.8	1.49	5.4	0.48	2
11	ESO 357-G26	R	-1.0	1362	18.3	89.6	79.4	7.04	38.2	3.39	16.2	1.44	1
12	ESO 418-G15	R	4.0	1068	13.9	90.0	105.2	7.09	34.7	2.34	9.7	0.65	2
13	NGC 1531/32	r	2.7	1190	16.0	90.0	308.0	23.89	96.0	7.45	38.0	2.94	2
14	ESO 202-G04	R	2.0	990	14.7	90.0	40.7	2.90	8.4	0.60	7.2	0.51	2
15	ESO 362-G11	R	4.0	1348	19.0	88.0	104.2	9.60	31.7	2.92	13.5	1.24	1
16	NGC 1888	r	5.0	2432	31.8	90.0	96.8	14.92	25.6	3.95	12.3	1.89	2
		K'	5.0	2432	31.8	90.0	62.3	9.60	14.9	2.29	8.3	1.27	2
17	ESO 363-G07	R	5.5	1324	18.9	89.0	96.7	8.86	32.7	3.00	10.7	0.98	1
18	ESO 487-G35	R	7.8	1731	23.6	90.0	74.4	8.51	27.8	3.18	9.7	1.11	2
19	NGC 2188	r	9.0	749	11.6	90.0	183.2	10.30	35.2	1.98	20.3	1.14	1
		K'	9.0	749	11.6	90.0	79.3	4.46	38.9	2.19	13.3	0.75	2
20	UGC 3697	R	7.0	3137	43.5	90.0	65.2	13.75	29.0	6.11	3.0	0.62	2
		H	7.0	3137	43.5	90.0	73.2	15.44	22.2	4.68	5.7	1.21	2
21	ESO 060-G24	r	2.5	4096	57.6	87.0	97.5	27.23	19.9	5.55	6.8	1.89	2
22	ESO 497-G14	R	3.0	3446	45.4	90.0	45.6	10.04	17.4	3.82	5.9	1.29	2
23	NGC 2820	H	5.0	1580	31.2	90.0	78.0	11.80	19.2	2.90	7.8	1.18	2
24	NGC 3044	r	5.0	1292	21.4	89.0	179.2	18.59	40.0	4.15	10.6	1.10	1
		K'	5.0	1292	21.4	89.0	89.9	9.33	27.6	2.86	7.9	0.82	2
25	NGC 3187	r	5.0	1578	25.0	86.0	148.0	17.94	26.0	3.15	27.9	3.39	1
		K'	5.0	1578	25.0	86.0	84.2	10.21	62.3	7.55	18.3	2.22	2
26	ESO 317-G29	R	1.0	2520	34.6	90.0	71.9	12.06	24.8	4.16	11.5	1.93	2
27	ESO 264-G29	R	5.6	3310	45.6	90.0	42.7	9.43	13.9	3.07	4.3	0.94	2
		K'	5.6	3310	45.6	90.0	38.2	8.45	8.5	1.88	2.5	0.55	2
28	NGC 3432	R	9.0	616	10.5	90.0	119.6	6.09	29.0	1.48	14.3	0.73	1
		K'	9.0	616	10.5	90.0	112.3	5.72	64.2	3.27	16.7	0.85	1
29	NGC 3628	r	3.0	847	4.8	88.0	432.0	10.05	400.0	9.31	68.0	1.58	2
		K'	3.0	847	4.8	88.0	231.0	5.38	96.2	2.24	31.4	0.73	1
30	ESO 378-G13	R	1.0	—	—	90.0	32.2	—	19.8	—	4.3	—	2
		K'	1.0	—	—	90.0	31.9	—	29.7	—	3.3	—	3
31	ESO 379-G20	R	1.0	14400	193.1	90.0	48.6	45.48	14.9	13.92	3.1	2.94	2
		K'	1.0	14400	193.1	90.0	44.6	41.73	12.7	11.92	3.3	3.12	2
32	NGC 4183	R	6.0	932	17.6	90.0	137.8	11.76	39.9	3.40	8.7	0.74	2
		R	6.0	932	17.6	90.0	78.3	6.68	39.9	3.40	7.6	0.65	2
		K'	6.0	932	17.6	90.0	88.5	7.55	38.5	3.28	12.7	1.08	1
33	NGC 4631	R	7.0	606	8.0	89.0	261.0	10.12	79.8	3.09	27.4	1.06	1
		K'	7.0	606	8.0	89.0	241.0	9.33	54.5	2.11	22.5	0.87	2
34	NGC 4634	r	6.0	160	15.8	89.5	83.8	6.42	27.3	2.09	8.8	0.67	1
		K	6.0	160	15.8	89.5	65.0	4.98	16.5	1.26	6.0	0.46	1
35	NGC 4747	R	6.0	1188	22.4	88.0	79.8	8.66	20.3	2.20	13.6	1.47	1
36	NGC 4762	r	-2.0	985	11.7	87.0	272.0	15.43	164.0	9.30	23.1	1.31	2
		r	-2.0	985	11.7	89.0	118.0	6.69	164.0	9.30	15.1	0.86	1
		K'	-2.0	985	11.7	89.0	160.4	9.10	128.3	7.28	11.4	0.65	3
		K'	-2.0	985	11.7	89.0	119.3	6.77	128.3	7.28	12.0	0.68	1

Table 5. (continued)

No.	Galaxy	Band	Type	v_0	Dist	i	$R_{\max}$		h		z_0		$f(z)$
				[km s^{-1}]	[Mpc]	[°]	["]	[kpc]	["]	[kpc]	["]	[kpc]	
(1)	(2)	(3)	(4)	(5)	(6)	(7)	(8)		(9)		(10)		(11)
37	ESO 443-G21	r	6.0	2798	38.3	90.0	72.0	13.37	16.0	2.97	5.3	0.98	2
		K'	6.0	2798	38.3	90.0	43.9	8.15	22.7	4.21	4.0	0.74	2
38	NGC 5126	R	0.0	4727	64.2	89.0	40.7	12.66	14.9	4.63	6.6	2.07	2
39	ESO 324-G23	r	6.5	1443	26.7	89.5	103.2	13.36	31.2	4.04	16.7	2.16	1
		K'	6.5	1443	26.7	89.5	74.2	9.60	35.0	4.53	8.5	1.10	2
40	ESO 383-G05	r	3.7	3626	50.0	89.0	108.4	26.28	33.9	8.22	13.5	3.28	1
41	NGC 5297	R	4.5	2407	37.9	90.0	61.6	11.32	19.6	3.60	10.2	1.88	2
42	ESO 445-G63	r	5.3	—	—	90.0	52.6	—	10.1	—	6.4	—	2
43	NGC 5529	R	5.0	2883	37.0	87.5	132.0	23.68	23.2	4.16	6.8	1.22	1
		H	5.0	2883	37.0	87.5	114.0	20.45	48.0	8.61	8.0	1.44	2
44	NGC 5965	R	3.0	3412	45.8	86.5	106.6	23.67	27.6	6.12	8.9	1.98	1
45	NGC 6045	R	5.0	10049	133.3	87.0	31.2	20.16	15.1	9.75	5.5	3.55	1
		K	5.0	10049	133.3	90.0	23.7	15.30	22.4	14.48	3.5	2.26	2
46	NGC 6361	R	3.0	3812	53.1	90.0	69.2	17.82	21.1	5.44	11.0	2.83	1
		nf[a)]	3.0	3812	53.1	90.0	80.8	20.79	18.6	4.79	10.8	2.78	2
		K	3.0	3812	53.1	90.0	23.7	6.10	22.4	5.77	6.1	1.57	2
47	Arp 121	R	2.0	5489	75.1	90.0	42.8	15.57	20.1	7.33	5.8	2.10	2
		K	2.0	5489	75.1	90.0	32.0	11.65	11.5	4.19	4.4	1.61	2
48	ESO 462-G07	K'	4.0	—	—	90.0	33.3	—	10.6	—	3.1	—	2
49	IC 4991	r	-2.0	5660	79.9	90.0	39.2	15.18	12.0	4.65	2.5	0.97	3
						Non – Interacting							
1	UGC 231	R	6.0	842	13.7	90.0	82.5	5.48	39.6	2.63	5.3	0.35	3
		K	6.0	842	13.7	90.0	62.7	4.17	33.3	2.21	6.1	0.41	3
2	ESO 150-G07	r	1.0	—	—	90.0	29.5	—	6.9	—	3.4	—	2
3	ESO 112-G04[b)]	r	5.6	—	—	87.5	45.0	—	22.7	—	2.0	—	2
4	ESO 150-G14[b)]	r	0.4	8257	114.4	90.0	64.0	35.52	23.3	12.93	5.2	2.87	2
5	UGC 711	R	6.7	1979	27.0	90.0	85.3	11.17	35.7	4.67	6.2	0.82	2
6	ESO 244-G48	r	3.0	—	—	87.0	45.3	—	13.5	—	6.9	—	1
7	UGC 1839	R	7.3	1536	20.7	90.0	75.4	7.57	22.6	2.27	6.8	0.69	2
8	NGC 891	R	3.0	528	9.5	89.4	365.4	16.83	165.0	7.60	23.6	1.09	2
		K'	3.0	528	9.5	89.4	336.8	15.51	99.4	4.58	14.9	0.69	1
9	ESO 416-G25[b)]	r	3.0	4997	68.9	87.0	69.8	23.32	30.9	10.32	4.8	1.61	2
10	UGC 2411	R	8.5	2547	37.3	90.0	90.8	16.42	36.2	6.55	4.5	0.82	2
11	IC 1877	R	3.0	—	—	90.0	19.7	—	12.2	—	2.0	—	3
12	ESO 201-G22	R	5.0	4069	57.3	89.0	75.4	20.94	31.2	8.68	4.0	1.11	2
13	NGC 1886	R	3.5	1755	23.6	87.5	86.8	9.93	20.8	2.38	5.6	0.64	2
		K'	3.5	1755	23.6	87.5	78.3	8.96	22.5	2.57	6.1	0.70	1
14	UGC 3474	R	6.0	3634	50.5	89.0	47.3	11.59	23.2	5.68	3.8	0.94	2
		K'	6.0	3634	50.5	89.0	57.7	14.13	20.4	5.00	4.1	1.00	1
15	NGC 2310	R	-2.0	1187	18.4	90.0	103.1	9.20	26.3	2.35	10.2	0.91	2
16	UGC 4278	R	7.0	563	10.9	90.0	97.6	5.16	29.0	1.53	5.8	0.30	2
		H	7.0	563	10.9	90.0	168.0	8.88	48.0	2.54	9.9	0.52	2
17	ESO 564-G27[b)]	r	6.3	2178	33.2	87.0	131.4	21.15	34.1	5.50	4.0	0.64	2
18	UGC 4943	R	3.0	2265	34.2	90.0	50.2	8.33	12.1	2.00	1.7	0.29	2
		H	3.0	2265	34.2	90.0	49.2	8.16	10.8	1.79	2.9	0.48	2
19	IC 2469	r	2.0	1666	22.2	82.0	197.0	25.79	45.2	5.92	13.9	1.50	1
20	UGC 5341	R	6.0	7568	97.3	89.0	86.8	40.95	31.7	14.97	4.2	2.00	2
		K'	6.0	7568	97.3	89.0	66.1	31.17	19.1	9.03	2.7	1.26	1
21	IC 2531	r	5.3	2477	33.0	89.2	220.0	35.20	67.2	10.75	9.8	1.57	2
22	NGC 3390	r	3.0	2820	37.9	89.0	113.1	20.78	23.4	4.30	9.2	1.69	1
23	ESO 319-G26[b)]	r	5.3	3601	42.4	89.5	51.8	10.65	14.3	2.93	2.0	0.41	3
24	NGC 3957	r	-1.0	1703	29.6	89.0	93.6	13.43	23.4	3.36	8.4	1.20	1
25	NGC 4013	R	3.0	839	12.0	89.5	96.4	5.61	24.6	1.43	11.6	0.67	1
		K'	3.0	839	12.0	89.5	117.4	6.83	43.6	2.54	9.7	0.57	1

Table 5. (continued)

No.	Galaxy	Band	Type	v_0	Dist	i	$R_{\max}$		h		z_0		$f(z)$
				[km s^{-1}]	[Mpc]	[°]	[″]	[kpc]	[″]	[kpc]	[″]	[kpc]	
(1)	(2)	(3)	(4)	(5)	(6)	(7)	(8)		(9)		(10)		(11)
26	ESO 572-G44	r	3.0	6759	89.9	89.5	50.4	21.95	33.1	14.41	6.5	2.82	1
27	UGC 7170	R	6.0	2444	29.7	90.0	54.1	7.79	16.4	2.36	2.8	0.41	2
28	ESO 321-G10[b)]	r	1.4	3147	42.4	88.0	64.0	13.17	25.8	5.31	4.8	0.99	1
29	NGC 4217	R	3.0	1026	14.6	89.0	150.8	10.67	29.0	2.05	21.6	1.53	2
30	NGC 4244	R	6.0	243	3.8	90.0	322.6	5.94	76.1	1.40	18.4	0.34	2
31	UGC 7321	R	7.0	409	15.8	90.0	103.4	7.92	44.4	3.40	4.7	0.36	2
		H	7.0	409	15.8	90.0	163.2	12.50	43.2	3.31	7.1	0.55	2
32	NGC 4302	R	5.0	1108	15.8	90.0	181.6	13.91	74.2	5.68	7.0	0.53	2
		H	5.0	1108	15.8	90.0	145.2	11.12	66.0	5.06	13.0	0.99	2
33	NGC 4330	r	6.0	1569	15.8	88.5	290.0	22.21	108.8	8.33	25.3	1.94	1
		K'	6.0	1569	15.8	88.5	95.6	7.32	39.6	3.04	7.9	0.60	2
34	NGC 4565	R	3.0	1227	10.0	88.0	229.4	11.12	67.6	3.28	10.8	0.52	1
		K'	3.0	1227	10.0	88.0	311.2	15.09	96.2	4.66	15.3	0.74	2
35	NGC 4710	R	-1.0	1119	14.4	87.0	134.1	9.36	39.9	2.78	18.0	1.25	2
		R	-1.0	1119	14.4	87.0	79.8	5.57	16.7	1.16	9.8	0.69	1
		K'	-1.0	1119	14.4	87.0	117.4	8.20	38.5	2.69	12.4	0.86	2
36	NGC 5170	r	5.0	1503	15.8	88.0	272.0	20.84	124.0	9.50	20.3	1.56	1
		H	5.0	1503	15.8	88.0	222.0	17.01	96.0	7.35	15.4	1.18	2
		K	5.0	1503	15.8	88.0	222.0	17.01	66.0	5.06	11.7	0.90	2
37	ESO 510-G18	r	1.0	—	—	90.0	16.4	—	3.8	—	1.2	—	2
38	UGC 9242	R	7.0	1440	25.2	88.5	93.7	11.45	41.1	5.02	4.7	0.57	1
		H	7.0	1440	25.2	88.5	70.4	8.60	19.2	2.35	1.8	0.22	3
39	NGC 5775	r	5.0	1681	28.9	87.0	127.1	17.81	31.2	4.37	13.1	1.84	1
40	NGC 5907	R	5.0	667	11.0	88.0	276.0	14.72	145.9	7.78	16.9	0.90	2
		H	5.0	667	11.0	88.0	225.6	12.03	48.0	2.56	12.3	0.66	2
41	NGC 5908	R	3.0	3306	44.7	88.0	78.0	16.89	20.1	4.36	7.6	1.66	2
		K'	3.0	3306	44.7	88.0	78.9	17.10	24.3	5.26	7.4	1.61	1
42	ESO 583-G08	r	4.0	7451	101.4	86.7	53.4	26.27	12.5	6.14	1.8	0.88	2
43	NGC 6181	R	5.0	2375	36.0	90.0	30.4	5.31	13.0	2.28	4.6	0.80	2
44	ESO 230-G11	r	4.0	5258	69.0	89.0	38.8	12.99	15.0	5.01	4.2	1.42	3
45	NGC 6722[b)]	r	3.0	4626	66.3	87.5	84.6	27.19	24.0	7.73	7.3	2.34	1
46	ESO 461-G06	r	5.0	—	—	88.8	60.8	—	16.0	—	3.0	—	1
47	ESO 339-G16[b)]	r	1.0	—	—	87.0	45.7	—	11.4	—	4.0	—	2
48	IC 4937[b)]	r	3.0	−84	63.0	89.8	75.6	23.08	27.3	8.33	6.7	2.04	2
49	ESO 187-G08	r	6.0	4374	63.1	90.0	55.8	17.07	14.8	4.52	3.2	0.98	3
50	IC 5052	r	7.0	591	8.0	89.5	200.9	7.79	48.8	1.89	19.8	0.77	1
		K'	7.0	591	8.0	89.5	135.9	5.27	67.3	2.61	11.9	0.46	2
51	IC 5096	r	4.0	3087	45.9	87.0	95.4	21.22	32.3	7.20	6.5	1.46	1
52	ESO 466-G01[b)]	r	2.0	7095	98.7	88.0	56.1	26.86	13.2	6.30	7.7	3.67	1
53	ESO 189-G12	r	5.0	8370	116.3	88.0	55.8	31.46	23.0	12.99	3.8	2.16	1
54	UGC 11859[b)]	r	4.0	3014	45.1	88.0	106.9	23.38	25.2	5.51	1.5	0.32	1
55	ESO 533-G04	r	4.8	2569	38.2	87.0	74.9	13.87	25.2	4.67	6.7	1.24	1
56	IC 5199	r	3.0	5037	71.5	86.5	58.5	20.28	17.6	6.08	4.5	1.57	1
57	UGC 11994	R	4.0	4872	70.6	90.0	70.1	24.00	14.8	5.08	2.3	0.80	3
58	UGC 12281	R	8.0	2567	39.5	90.0	103.1	19.75	40.2	7.71	6.0	1.16	2
		K	8.0	2567	39.5	90.0	56.3	10.79	25.6	4.90	5.1	0.98	1
59	UGC 12423	R	5.0	4839	70.0	87.4	100.6	34.14	25.1	8.54	6.6	2.23	1
		K	5.0	4839	70.0	87.4	53.8	18.24	17.9	6.08	4.0	1.70	2
60	NGC 7518	R	1.0	3536	52.6	87.0	55.1	14.05	13.0	3.33	7.6	1.93	1
61	ESO 604-G06	r	4.0	7665	106.1	89.6	74.9	38.52	22.6	11.64	3.0	1.54	2

[a)] nf=no filter used.

[b)] Supplementary data from Barteldrees & Dettmar (1994).